

AN ANALYTICAL APPROACH TO THE COMPLETE MOMENT-CURVATURE CURVE OF RECTANGULAR REINFORCED CONCRETE COLUMNS

R. Hachem & B. Bousalem

Civil Engineering Department, LMDC, Constantine University, 25000, Constantine, Algeria

ABSTRACT

As part of continuing research study, this paper proposes a sectional ductility analyze on rectangular reinforced concrete columns under large inelastic deformations while simultaneously subjected to constant axial load. In order to estimate the flexural behavior of reinforced concrete members, the stress strain behavior of the constituent materials must be well established. Various analytical models available in the literature for confinement concrete by different types of transverse reinforcement including the one used in the present analyze are proposed.

The purpose is to draw the complete analytical moment-curvature curve for reinforced concrete columns. A parametric investigation is conducted for examining the effects of various variables on moment-curvature relationships such as the amount of transverse and longitudinal steel, and the level of the compression force. The experimental and analytical results are being compared and the final conclusions are made

Key words : moment-curvature curve - columns - reinforced concrete

RESUME

En tant qu'élément d'une recherche continue, cet article propose une analyse de ductilité de section des poteaux confinés en béton de section rectangulaire sous de grandes déformations inélastiques simultanément soumis à une charge axiale constante. Afin d'estimer le comportement flexionnel des éléments en béton armé, le comportement contrainte-déformation des matériaux constitutifs doit être bien établi. On propose les divers modèles analytiques disponibles dans la littérature pour le béton confiné par différents types d'acier transversal comprenant celui utilisé dans la présente analyse.

L'objectif est de tracer la courbe analytique complète moment-courbure pour les poteaux en béton armé. Une investigation paramétrique est conduite pour examiner l'influence de certains paramètres notamment les taux d'aciers de confinement et de résistance, l'intensité de l'effort normal et. Les résultats expérimentaux et analytiques sont confrontés et des conclusions finales sont tirées.

Mots clés : courbe moment-courbure – Poteau – béton armé

INTRODUCTION

Though it is commonly recommended in well established codes that columns subjected to lateral forces such as seismic loads must be designed according to the displacement or recently performance based approach; The most important design consideration for ductility in plastic hinge region of reinforced concrete columns is the provision of transverse reinforcement that has a double function in resisting shear forces as well as providing confinement to the concrete core [1, 2]. Tests have shown that the confinement of concrete by adequate arrangement of transverse reinforcement will cause a significant enhancement in the flexural strength capacity of the reinforced concrete column. It appears that the newly edition of the RPA [3] on the subject is still not suitable to provide the necessary lateral steel content required for a given ductility demand.

The objective of this is paper is to develop the complete moment-curvature curve for rectangular reinforced concrete columns based on sectional ductility analysis in order to verify the quantity of the confining steel required in reinforced concrete columns sections to achieve the ultimate curvatures required in seismic design for ductility demands. Experimental behaviour of specimen tested by Sheikh and Yeh [4] and analytical results considering Mander model were compared. The unconfined moment capacity is calculated based on the equivalent rectangular concrete stress block recommended by the CBA93 [5].

ANALYTICAL STRESS-STRAIN CURVES OF CONFINED CONCRETE

Various stress-strain models for the prediction of the confined concrete have been proposed [6-8]. Almost all analytical models were developed in the

light of the experimental data. The following section provides a summary of some analytical models.

Sheikh and Uzumeri [6]

The proposed model assume that the effectively confined concrete area is less than the core area and is determined by introducing the effectiveness confinement coefficient that takes in account the distribution of longitudinal steel, the tie configuration and the spacing of ties. The complete stress-strain curve was calibrated against their own test results.

Modified Kent and Park [7]

Park *et col.* modified the original model by making an allowance for the enhancement in the concrete strength and the peak strain due to confinement. The increase in strength and the corresponding strain was assumed to be equal to $\rho_s f_{yh}$. The slope of the descending part of the curve remained the same as in the original model up to a stress of 20 % of the maximum, beyond which a horizontal line represented the curve.

Hoshikuma *et col.* [8]

The stress strain model was based on the results of a series of compression loading tests of reinforced concrete columns with various shapes and reinforcement arrangements so as to cover practical bridge column sections designed in Japan. The experimental results have shown that the three parameters that define the proposed model -peak stress, peak strain and deteriorating rate- were significant factors for the stress strain curve of confined concrete.

EXPERIMENTAL INVESTIGATION

Experimental evidence of a total of 90 compressed reinforced concrete columns confined by either circular or rectangular transverse lateral steel was selected and investigated herein and used to determine a representation of the stress strain relationship of confined concrete. A summary of this previous experimental work, with details of specimens and variables considered is given in Table1.

ANALYTICAL STRESS-STRAIN MODEL ADOPTED

One of the available stress-strain models for confined reinforced concrete sections is chosen in this study to be used in generating the moment-curvature curves for reinforced concrete columns. The chosen model was proposed by Mander *et*

col. [12] is illustrated in figure 1. The major parameters in the concrete stress-strain curve are effective lateral confining pressure, f'_l and confined concrete strength, f'_{cc} , which are expressed in equations (1) and (2), respectively.

$$f'_l = \frac{1}{2} K_e \rho_s f_{yh} \quad (1)$$

$$f'_{cc} = f'_{co} \left(-1,254 + 2,254 \sqrt{1 + \frac{7,94 f'_l - 2 f'_l}{f'_{co}}} \right) \quad (2)$$

The parameter K_e in equation (1) is the ratio of the smallest effectively confined concrete core area, which is located midway between two layers of confining steel, to the nominal concrete core area, which is measured to the centre line of the confining steel. The effectively confined concrete core area is obtained by assuming that the core concrete spalls in the form of a series of second-degree parabolas between the clear distance of the longitudinal steel bars supported by the corner of a hoop or cross tie in the horizontal plane, and between the clear spacing of the confining steel in the vertical plane with an angle of 45°. The following equation expressed K_e for rectangular confinement :

$$K_e = \frac{\left(1 - \sum_{i=1}^n \frac{(w_i')^2}{6b_c d_c} \right) \left(1 - \frac{S'}{2b_c} \right) \left(1 - \frac{S'}{2d_c} \right)}{(1 - \rho_{cc})} \quad (3)$$

The strain corresponding to the peak stress is expressed as:

$$\varepsilon_{cc} = \varepsilon_{co} \left[1 + 5 \left(\frac{f'_{cc}}{f'_{co}} - 1 \right) \right] \quad (4)$$

The entire confined concrete stress-strain relationship is expressed following the Popovics model [13] in the form of:

$$f_c = \frac{f'_{cc} x r}{r - 1 + x^r} \quad (5)$$

$$\text{Where: } x = \frac{\varepsilon_c}{\varepsilon_{cc}}, \quad r = \frac{E_c}{E_c - E_{sec}}, \quad E_{sec} = \frac{f'_{cc}}{\varepsilon_{cc}}$$

for confined concrete and $\frac{f'_{co}}{\varepsilon_{co}}$ for unconfined concrete.

The reasons for adopting the modified Mander *et col.* concrete stress-strain model are:

- Only one single equation defines both the ascending and descending branches of the stress-strain curve;
- The model can also be used for unconfined concrete sections;

(c) The model can be applied to any shape of concrete member section confined by any kind of transverse reinforcement (spirals, cross ties, circular or rectangular hoops); (d) There is no residue stress at the tail end of the stress-strain curve.

The last phenomenon resembles more the behavior of confined concrete under compression at large deformation.

Ultimate compressive strain

Scott *et col.* [14] observed that it is reasonably conservative to define the limit of useful concrete compressive strain ϵ_{cu} , where the first hoop fractures occurs. Recently, Priestley *et col.* [15] proposed a value of ϵ_{cu} based on energy balanced approach and is given by the following expression:

$$\epsilon_{cu} = 0.004 + 1.4 \frac{\rho_s f_{yh} \epsilon_{sm}}{f_{cc}'} \quad (6)$$

ANALYTICAL MOMENT – CURVATURE CURVES

Using the stress strain curve for concrete [12], and the stress strain model for longitudinal reinforcement proposed by Mander *et col.* [16] as shown in figure 2, a series of analytical moment curvature curves can be generated taking into account the different influencing parameters.

Assumptions

The assumptions used in theoretical moment curvature analysis are as follows.

- Plane section before bending remain plane after bending,
- Tensile strength of concrete is ignored,
- Stresses in concrete are derived from the appropriate stress strain curves respectively for confined and unconfined concrete
- Stresses in longitudinal reinforcement are derived from the stress strain curve using Mander model and experimental data including strain hardening
- Perfect bond between steel and concrete
- In the application of the analytical models, the lateral steel stress is suggested to be equal to yield stress
- The ultimate state is reached when one of the three limit is attained:
 1. the concrete strain at the extreme compression fibre reaches the specified value ϵ_{cu} ,
 2. the steel strain in the tension zone reaches the specified value ϵ_{su} ,

3. the flexural moment drops to a value of $0.8 M_{max}$.

4. the concrete strain at the extreme compression fibre reaches the specified value ϵ_{cc} in the case of compression.

Procedure

Based on these assumptions, a computer program “**Hoop**” was developed to carry out calculations for confined and unconfined sections with any type arrangement of reinforcement. Moreover, the program can switch between two output functions, the first giving the $M-\phi$ data and also the strains of concrete and steel considered after every iteration, and the second, giving the ductility of the section considering the yield and the ultimate curvature values, as well as the corresponding moments. The program flowchart is illustrated in figure 3.

To determine the moment curvature relationships, the following procedure is used:

the section is divided into a number of discrete laminas having the orientation of the neutral axis depth; each one is formed by two kinds of concrete, core and cover:

- a) Assign an initial value of compressive strain at extreme concrete fiber.
- b) Assume a neutral axis depth.
- c) Calculate the strain and the corresponding stress at the centroid of each longitudinal reinforcement bar level.
- d) Calculate the strain at the middle of each discrete lamina and the associated stress.
- e) Determine the internal forces by summing the lamina contributions and the steel forces in different levels.
- f) Calculate the axial force from equilibrium and compare with the applied axial load. If the difference is less than or equal to a specified tolerance, results are acceptable and moment curvature values are computed. Otherwise, adjust neutral axis depth and return to step d. If convergence does not occur in 500 iterations, assign a new concrete strain and return to step c, the procedure is well explained in figure 4.

Comparison of analytical and experimental moment curvature relationships

The theoretical moment-curvature relationships are compared with experimental data reported by Sheikh *et col.* (Specimen A3) [4], the results showed that analytical moment-curvature curve is close to the experimental one, as illustrated in figure 5.

Parametric study

The effect of different variables is studied by comparing moment curvature relations of the column sections in which only one major variable differed significantly. These variables included the level of axial load, the amount of both transverse and longitudinal steel. The configuration with a single interior hoop is chosen in this study and kept constant for all the study, this type is commonly used in Algerian framed structures. All the moment curvature curves are obtained based on the assumed concrete section described in figure 6 using variables of table 2.

Level of axial load

Figure 7 illustrates the effect of axial load on moment curvature relationship. The level of axial load simulates the column axial load from medium to high stories. This level is defined as p equal to $P/f'_{co}A_g$ where P is the compressive axial load on the columns. It is observed that the ductility reduces as a result of higher axial load levels, and the moment beyond the maximum point degrades more rapidly as the level of axial load increases.

Amount of lateral reinforcement

The effect of this variable is clearly evaluated by comparing the behaviour of the three curves shown in Figure 8. The identical ascending parts of the curves indicate that the quantity of transverse steel do not influence the section behaviour prior to the first cracking of unconfined concrete. It can be noticed that the ductility increases with the increase of transverse steel content. It is apparent that with lower lateral volumetric ratios, the confining pressure is not sufficient enough to maintain the moment capacity of the section.

Amount of longitudinal reinforcement

Figure 9 illustrates the effect of longitudinal steel content on the moment curvature curve. It is demonstrated that the increase of the moment capacity of the section with the increase of the amount of longitudinal steel is small. The post peak behaviour is characterised by gradual drop in the moment capacity of the section where it reaches approximately a same value at ultimate curvatures. However a large longitudinal steel content means that less reliance is placed on the concrete capacity, and therefore the moment capacity can be better maintained at high curvatures.

Comparative study

Moment capacities and ductility values

Table 3 represents the experimental moment capacities of four representative columns along with ductility values. It can be seen that the

theoretical moment capacity (M_{CBA}) is based on the unconfined concrete strength (f'_{co}), and a maximum strain of the extreme compressed concrete fiber of 0.0035. With reference to CBA code, the strength enhancement beyond the M_{CBA} attains nearly a double. This is mainly due to the contribution of the confinement that is not allowed for in the CBA code on one hand and the value of the maximum concrete stress of the unconfined concrete which taken as $0.57 f'_{co}$ on the other hand.

The results indicated in Table 4 reveal that almost all the moment capacities and ductility values predicted by the present analyze are in well correlation with the experimental ones.

CONCLUSION

The conclusions reached from this analysis for the range of variables considered in this study are as follows:

1. The large transverse steel content and reduced tie spacing increase the ductility and enable the moment capacity to be better maintained at high curvatures.
2. The level of axial load reduces the ductility and the moment beyond the maximum point degrades more rapidly as the level of axial load increases.
3. The increase of the amount of longitudinal steel on the moment capacity of the section is small. However a large longitudinal steel content means that less reliance is placed on the concrete capacity, and therefore the moment capacity can be better maintained at high curvatures.
4. The moment capacity can increase significantly depending on the amount of confining steel and the magnitude of the axial compressive load, this enhancement will increase shear demand which might cause a brittle failure, to prevent this form happening confined moment capacity must be used instead of the unconfined one in determining the shear reinforcement in the column, this work if completed by a regression analyze can give an equation of the confined moment capacity.
5. The present RPA 99 code must include in its recommendations an expression for the quantity of transverse steel required in reinforced concrete column sections to achieve the ultimate curvatures required in seismic design for ductility.

REFERENCES

- [1]. Bousalem B. *et col.* "Performance Parasismique des Portiques en Béton: Aspect Théorique de l'Approche en Capacité et Constat Réglementaire; Confinement des zones critiques dissipatives d'énergie", Revue Algérie EQUIPEMENT, 2001, 2^{ième} Partie : N°35.
- [2]. Hachem R., Bousalem B., Chikh N. "Ductilité De Courbure Des Poteaux En Béton Armé De Section Rectangulaire", Séminaire National de génie civil, Constantine, 08-09 Décembre 2004.
- [3]. Règlement Parasismique Algérien, RPA 99, CGS, Alger, Janvier. 2000.
- [4]. Sheikh S.A. and Yeh. C. "Tied Concrete Columns Under Axial Load And Flexure", Journal of structural engineering, October 1990, Vol. 116, N°10, pp.2780 -2800.
- [5]. CBA 93, Code du Béton Algérien, CGS, pp.23-24, Alger, Octobre 1993.
- [6]. Sheikh S.A., Uzumeri S.M., "Analytical Model for Concrete Confinement in Tied Columns". Journal of Structural Division, December 1982, Vol.108, N°ST12, pp.2703-2723.
- [7]. Park R. *et col.* "Ductility of Square Confined Concrete Columns", Journal of Structural Engineering, April 1982, Vol.108, N°4, pp.929-950.
- [8]. Hoshikuma J. *et col.*, "Stress-Strain Model for Confined RC in Bridge Piers", Journal of Structural Engineering, May 1994, Vol.123, N°5, pp. 624-633.
- [9]. Sheikh S.A., Uzumeri S.M., "Strength and Ductility of Tied Columns", Journal of Structural Division, May 1980, Vol.106, N°ST5, pp. 1079-1102.
- [10]. Moehle J. P. and Cavanagh T., "Confinement Effectiveness of Crossties in RC", Journal of Structural Engineering, October, 1985, Vol.111, N°10, pp. 2105-2120.
- [11]. Mander J.B. *et col.*, "Observed Stress-Strain Behaviour of Confined Concrete", Journal of Structural Engineering, 1988, Vol.114, N°8, August, pp. 1827-1849.
- [12]. Mander J.B. *et col.*, "Theoretical Stress-Strain Model for Confined Concrete", Journal of Structural Engineering, August 1988, Vol.114, N°8, pp. 1804-1826.
- [13]. Popovics S., "A Numerical Approach to the Complete Stress-Strain Curve Concrete", Cement and Concrete Research, 1973, Vol. 3, pp. 583-599.
- [14]. Scott B. D., Priestley M. J. N and Park R., "Stress-strain behavior of concrete confined by overlapping hoops at low and high strain rates", ACI Journal, January. February, 1982, pp. 13-27.
- [15]. Priestley M. J. N., Seible F. and Calvi G. M., "Seismic design and retrofit of bridges", John Wiley, 1996, pp. 686.
- [16]. Mander J. B., Priestley M. J. N. and Park R., "Seismic design of bridge piers", Department of civil engineering, University of Canterbury, 1984, Research report 84-2, pp. 483.

NOTATIONS

A_g	: gross area of cross-section
b_c, d_c	: concrete core dimensions measured to the center line of the perimeter tie
E_c, E_{sec}	: initial tangent modulus and secant modulus of concrete at peak stress respectively.
E_{sh}, E_s	: Young and strain hardening modulus of reinforcing steel respectively
f'_{co}, f'_{cc}	: compressive strength of unconfined and confined concrete respectively
f'_l, f_{yh}	: lateral confining stress and yield strength of confining steel respectively
f_c, f_s	: stress of concrete and reinforcing steel respectively
f_y, f_{su}	: yield and ultimate stress of reinforcing steel respectively
K_e	: confinement effectiveness coefficient
M_y, M_{max}, M_u	: Yield, maximum and ultimate moment respectively
N_{bt}	: number of laterally supported longitudinal bars
P	: axial load level
s'	: clear spacing between confining steel
w_i'	: clear distance between each longitudinal steel bar supported by the corner of a hoop or cross tie.
$\epsilon_{co}, \epsilon_{cc}$: the strain at peak stress of unconfined and confined concrete respectively
ϵ_{cu}	: ultimate confined concrete strain corresponding to first hoop fracture
ϵ_c, ϵ_s	: strain in concrete and reinforcing steel respectively
ϵ_{sm}	: ultimate transverse steel strain
$\epsilon_y, \epsilon_{sh}, \epsilon_{su}$: yield strain, strain at the onset of strain hardening, ultimate strain of reinforcing steel respectively
ϕ_l	: longitudinal bar diameter
ϕ_t	: transverse bar diameter
ϕ_y, ϕ_u	: Yield and ultimate curvature respectively
μ_ϕ	: ductility value
ρ_{cc}	: ratio of longitudinal steel area to nominal concrete core area measured to centre line of confining steel
ρ_s	: volumetric ratio of confining steel measured to outside of confining steel
ρ_l	: ratio of longitudinal steel area to gross-section area

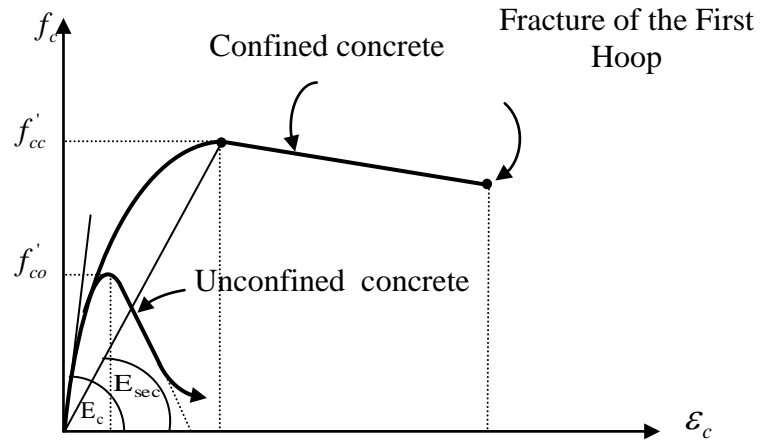


Figure 1: Stress Strain Curves for Confined Concrete Mander *et col.* (1988)

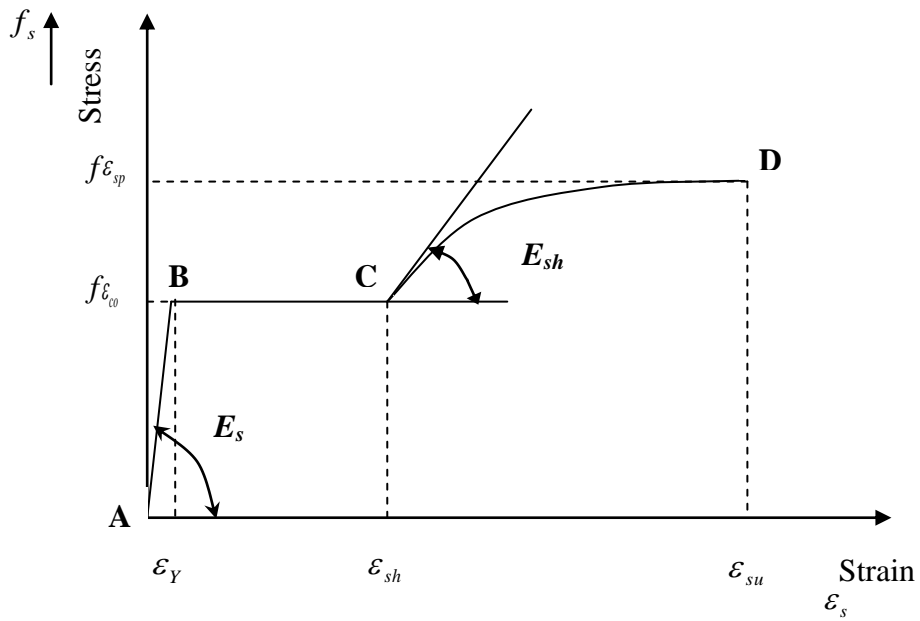
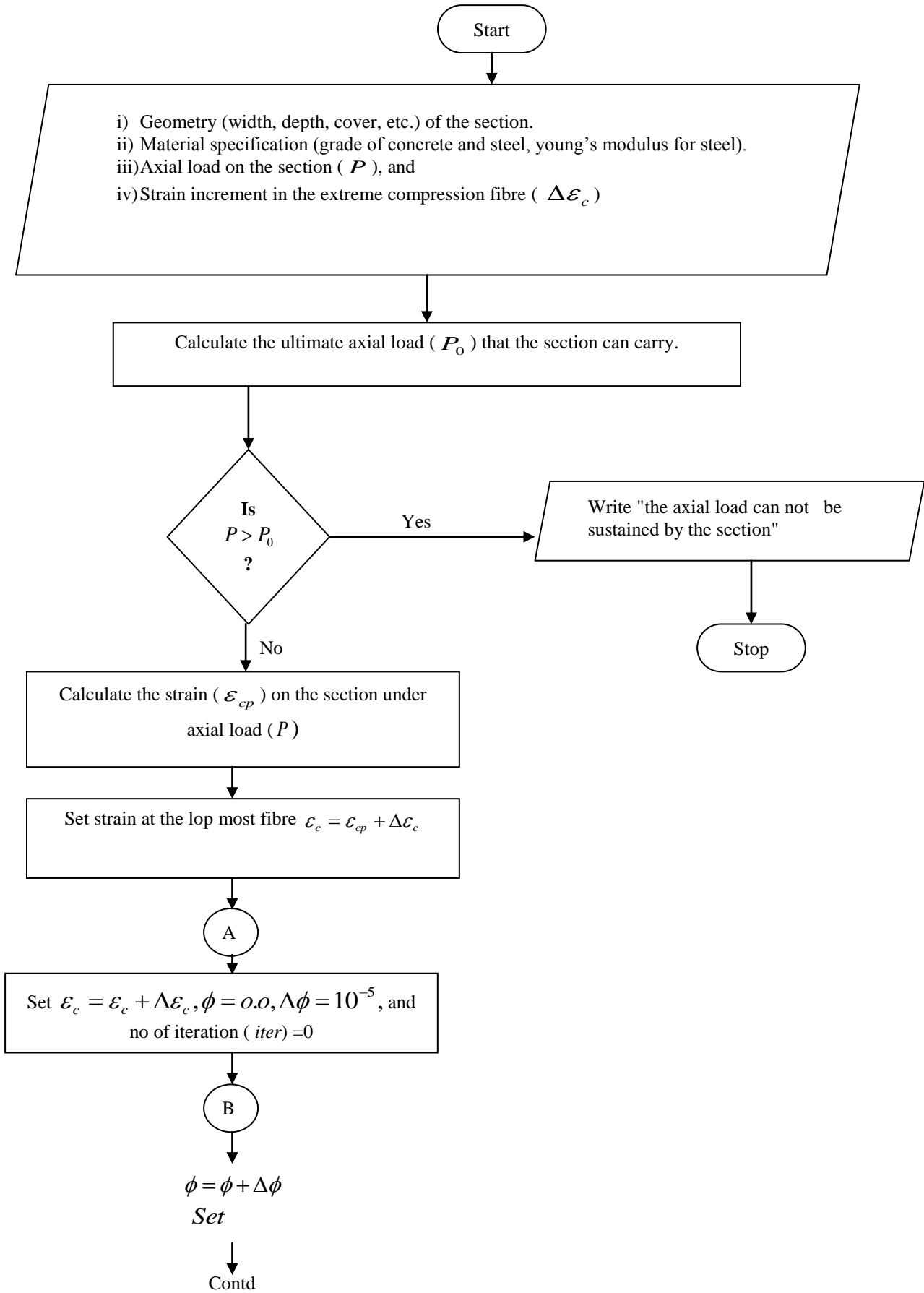


Figure 2: Stress Strain Curves for steel Mander *et col.* (1984)



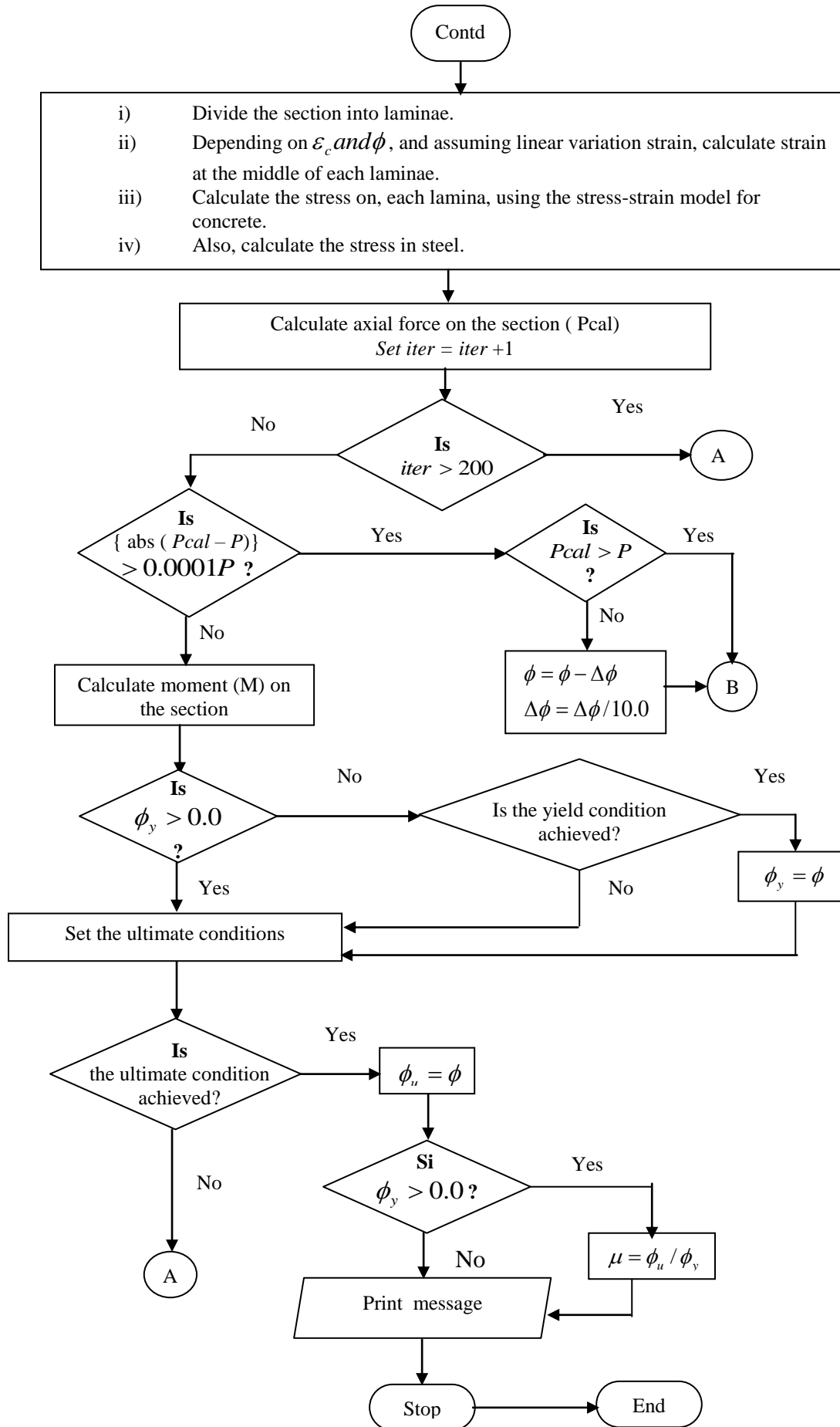


Figure 3: Flowchart of the software “Hoop”

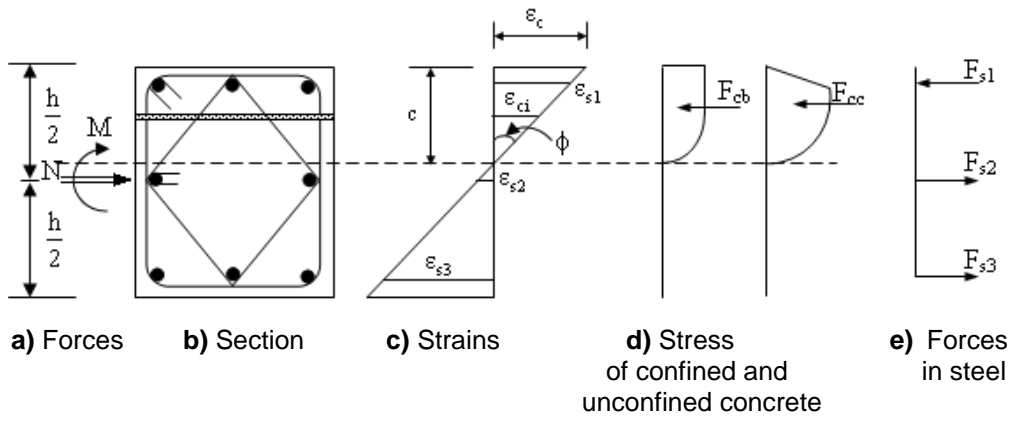


Figure 4: Moment-curvature Analyse

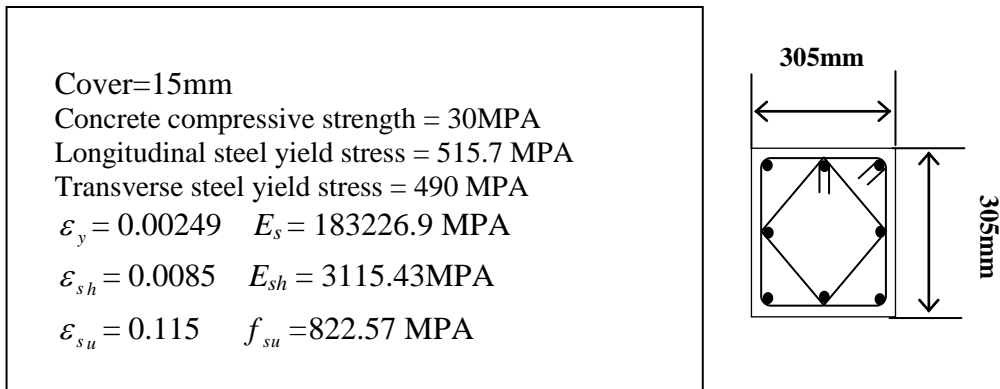


Figure 5: Properties of the Reinforced Concrete Section for the Parametric Study

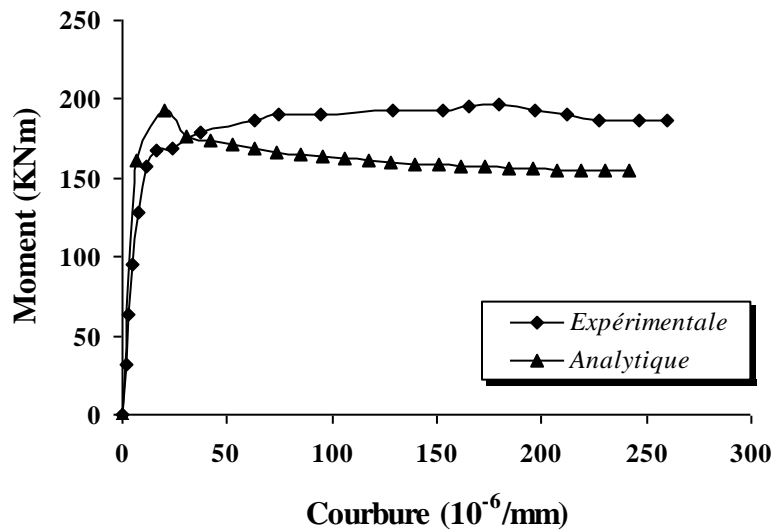


Figure 6: Comparison of Experimental and Analytical Curve for Specimens A3.

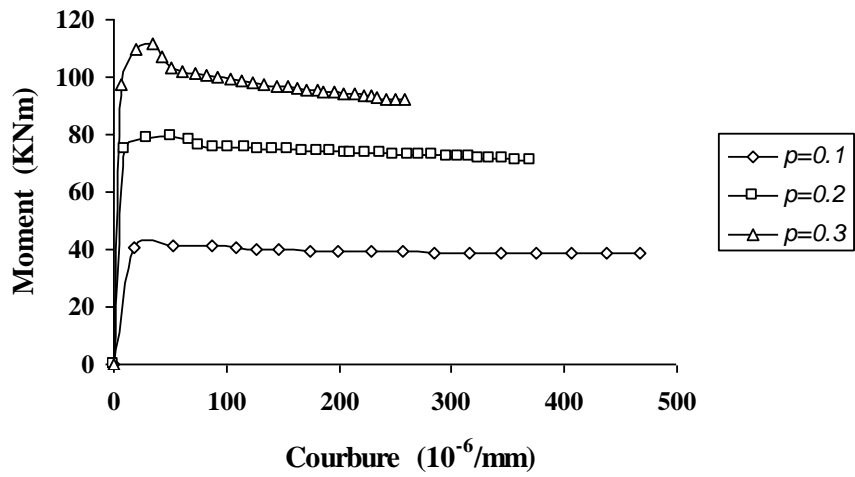


Figure 7: Effect of Axial Load Level

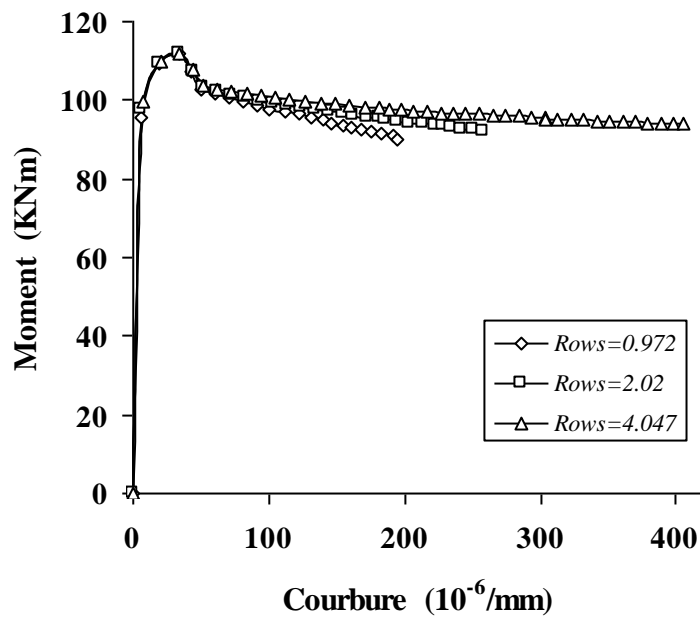


Figure 8: Effect of the Amount of Transverse Steel

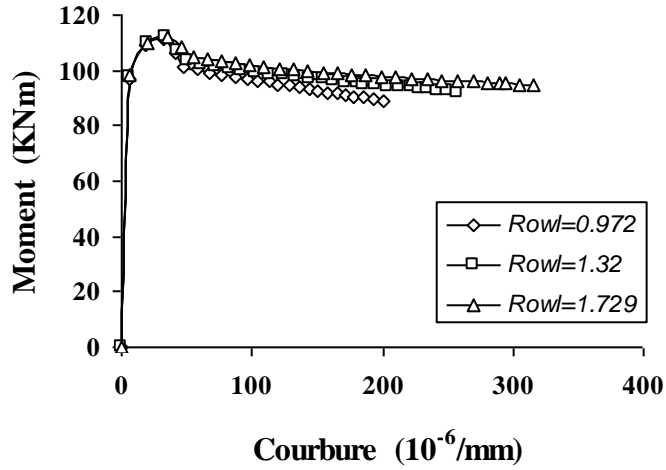


Figure 9: Effect of the Amount of Longitudinal Steel

Reference	Nb	Section (mm ²)	Test Specimen Parameters				
			ρ_l %	f'_{co} (MPa)	s' (mm)	ρ_s %	f_{yh} (MPa)
Sheikh <i>et col</i> [9]	24	305×305	2.2-4.8	26.6-34.8	29-102	0.76-2.4	265-798
Moehle <i>et col</i> [10]	8	305×305	2.44	32.3	38	1.21-2.07	440
Mander <i>et col</i> [11]	15	φ 450	1.23-3.7	24-32	36-119	0.6-2.5	307-340
	12	150×700	1.1-3.1	28-41	25-72	1.62-7.87	310-360
	6	φ 200	0	18.5	12.5-150	0.39-4.66	235
Hoshikuma <i>et col</i> [8]	10	φ 500	1.01	28.8	50-300	0.19-0.58	295
	6	200×200	0	23.2	12.5-150	0.39-4.66	235
	5	500×500	0.95	24.3	40-75	1.73-4.10	295
	1	350×700	0.97	24.3	65	1.72	295
	1	300×900	1.03	24.3	67	1.74	295
	2	250×1000	0.95	24.3	75	1.77-2.45	295

Table 1: Summary of Some Available Tests on Confined Concrete

Influent Parameters	$P = \frac{P}{f_{co}' A_g}$	Transverse Steel			Longitudinal Steel		
		ρ_s (%)	ϕ_t (mm)	s' (mm)	ϕ_l	ρ_l (%)	Nbt
Axial Load Level	0.1	2.02	10	100	14	1.32	8
	0.2						
	0.3						
Volumetric Ratio of Transverse Steel	0.3	4.047	10	50	12	0.972	8
		2.02	10	100			
		1.349	10	150			
Ratio of longitudinal Steel	0.3	2.02	10	100	12	0.972	8
					14	1.32	8
					16	1.729	8

Table 2: Values of Moment-curvature parametric study.

Specimen	M_y (kNm)		ϕ_y ($10^{-3}/m$)		M_{max} (kNm)		M_u (kNm)		ϕ_u ($10^{-3}/m$)		μ_ϕ	
	Th	Ex/Th	Th	Ex/Th	Th	Ex/Th	Th	Ex/Th	Th	Ex/Th	Th	Ex/Th
A3	182.00	0.86	13.32	1.32	192.60	0.87	154.54	1.21	233.31	1.11	17.52	0.84
E2	189.54	0.86	20.39	1.04	191.03	0.89	153.09	0.76	202.53	0.72	9.93	0.68
F4	182.87	1.01	13.50	0.80	193.22	1.02	155.27	1.20	234.04	1.11	17.34	1.40
D15	146.21	0.81	8.93	0.69	168.43	0.82	135.47	0.86	45.26	1.79	5.07	2.58
Average		0.86		0.96		0.90		1.01		1.18		1.38
Mean = 1.05, SD = 0.20												

$\rho_s = 1.68\%$ et $f_{yh} = 490$ MPa for all specimens.

Table 3: Experimental Ductility Values.

Specimen	(MPa)	ρ_1 (%)	P	M_y (kNm)	ϕ_y ($\times 10^{-3}/m$)	M_{max} (kNm)	M_u (kNm)	ϕ_u ($\times 10^{-3}/m$)	$\frac{M_{max}}{M_{CBA}}$	μ_ϕ
A3	31.8	2.44	0.61	157.2	17.6	168.0	186.6	259.4	1.396	14.7
E2	31.4	2.44	0.61	163.4	21.3	169.1	116.6	145.8	1.227	6.8
F4	32.2	2.44	0.60	184.5	16.2	196.5	186.0	202.2	1.394	12.5
D15	26.2	2.58	0.75	118.8	6.2	137.8	116.5	81	1.375	13.1

Table 4: Comparison of experimental and predicted ductility values